Relationship between Combustion Noise and Premixed Flame Behaviors in a Backward-Facing-Step Burner

Ji Hun Yeo and Nam Il Kim *
Department of Mechanical Engineering, Korea Advanced Institute of Science and Technology
Yuseong-gu, Daejeon, Republic of Korea

Abstracts

Backward-facing-step (BFS) structures have been used widely to investigate the combustion noise generated by the flame-vortex interaction. However, most studies were conducted using a few fixed step-width or nozzle-width. Thus, a BFS burner with continuously adjustable step-width was developed, and the characteristics of combustion noise were examined for C_3H_8 and CH_4 premixed flames. The combustion noise characteristics were classified into two modes: attached and lifted flames. The dependency of the maximal combustion noise on the flame modes was clearly distinguished, and a similar trend could be found regardless of fuels and compositions. After that, the flow field and flame behaviors were visualized and compared to understand the mechanism of flame-vortex interaction affecting combustion noise.

1 Introduction

Thermoacoustic instabilities and concerned combustion noises have been obstacles for various combustion systems. It is known that combustion instability occurs when the pressure and heat release fluctuation satisfy the Rayleigh Criteria [1]. Among various combustion instabilities, the interaction between the flame and vortex structure (flame-vortex interaction) can be a source of combustion noise. This noise can be self-sustained and results in harmonic peaks in the noise power spectrum [2]. Various experiments investigated flame-vortex interactions, and their characteristics were affected by the flame structure, which was varied by the vortex strength and size [3].

Meanwhile, the recirculation zone near a bluff body is widely used for flame stabilization (flame holder). However, the thermoacoustic instability often accompanies when the flame-vortex interaction repeatedly occurs in the recirculation zone [4]. In this study, a backward-facing-step (BFS) structure was selected, and the combustion noise on the BFS burner was observed. For the BFS structure, many experimental and numerical studies were also conducted. In these studies, it was reported that the combustion noise is affected by various complicated factors, such as the flame position, the laminar burning velocity (LBV), and the design configuration of the combustor [5,6].

Meanwhile, most previous experiments have been conducted using a few fixed step-width or nozzle-width, and the flow velocity or the equivalence ratios varied. However, such variation hindered our understanding because essential characteristics of flow and flame were varied at the same time. On the other hand, variation of the step-width and the nozzle-with of the BFS could distinguish the noise characteristics affected by the vortex size or the flow velocity [7,8].

Therefore, it will be helpful to examine the combustion noise with the variation of the step-width. In this study, a new BFS-burner was developed, of which the step-width could be varied continuously. Flame behavior and flow characteristics were visualized at the same time. Meanwhile, most previous studies

Correspondence to: dgandrew513@kaist.ac.kr

were focused on fully turbulent conditions for a better practical application. On the contrary, the characteristics of the flame-vortex interaction have been investigated mainly in the conditions of laminar conditions. Thus, this experiment was conducted in the transient regime between laminar and turbulent conditions to understand the mechanism between the flame-vortex interaction and the combustion noise.

2 Experimental methods

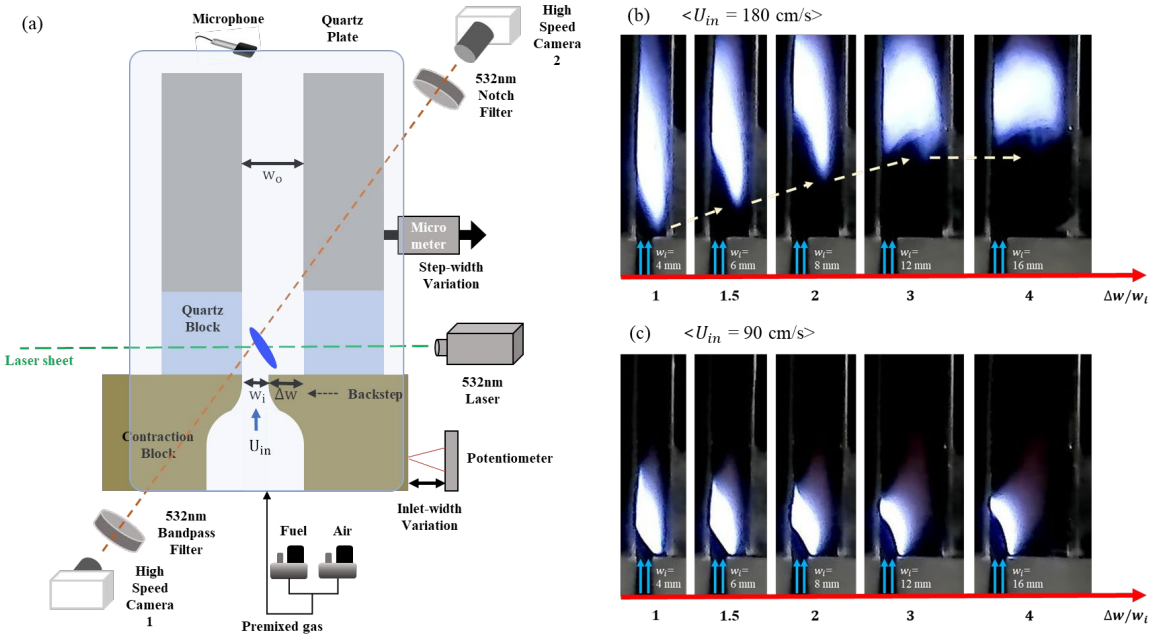

Figure 1: a) Experiment configuration and flame images of two different flame stabilization modes; b) Lifted flames and c) Attached flames (propane, $\phi = 0.9$, $w_i = 4$ mm).

The BFS-burner and the experimental setup are schematically described in Fig. 1a. Self-sustained combustion noise occurred when the flame was located above the BFS. The step-width (Δw) was controlled from 1 mm to 20 mm with a 1 mm distance. Combustion noise was measured using a microphone (130E20, PCB Piezotronics Inc.) at a fixed location near the outlet, and the noise power spectrum with respect to the frequency was analyzed. Above the contraction nozzle, two quartz blocks were installed between the two quartz plates so that a premixed flame could be formed within this channel and easily visualized. A laser sheet could be projected using a diode laser (532 nm), and the Mie scattering images could be obtained by introducing alumina particles (Al_2O_3) of 15 μm. Two high-speed cameras (Fastcam-Mini-UX100, Photron) were simultaneously used to capture the flame images and record the flow field. Premixed propane flames were mainly used at room temperature under atmospheric pressure, and premixed methane flames were partly used for comparison.

3 Results and Discussions

Prior to noise measurement, flame behaviors could be classified into two modes based on the flame front location, as shown in Fig. 1b and Fig. 1c; i.e., lifted flames and attached flames. The flame base was lifted from the nozzle when the flow velocity was sufficiently large, and the lift-off height of the flame base increased as the step-width increased. On the other hand, the flame base remained attached to the inlet at a small flow velocity, and the flame location was rarely affected by the step-width.

Combustion noise of propane premixed flames was measured with the variation of the step-width (Δw) and the inlet flow velocity (U_{in}). The noise power was defined as the maximum decibel value in the noise power spectrum, and its variation was depicted as a contour map, as shown in Fig. 2a. Overall, the specific step-width range of the significant noise power existed regardless of the equivalence ratios. While the step-width range proportionally increased with the flow velocity for the attached flames, it was maintained for the lifted flames. Meanwhile, the step-width where the strongest combustion noise ($\Delta w_{\max}$) occurred was depicted together, which has a similar trend with the specific step-width range.

At the three representative equivalence ratios ($\phi = 0.9, 1.1, 1.4$), variation of the combustion noise was examined, as shown in Fig. 2a. Average values of the critical step-width were marked with symbols, and their deviations at the same flow velocity were depicted an error bar. Solid symbols and hollow symbols correspond to the attached flames and the lifted flames, respectively. Notably, $\Delta w_{\max}$ gradually increased with U_{in} in the cases of attached flames at the low flow velocities. On the contrary, $\Delta w_{\max}$ was similar at the higher flow velocities.

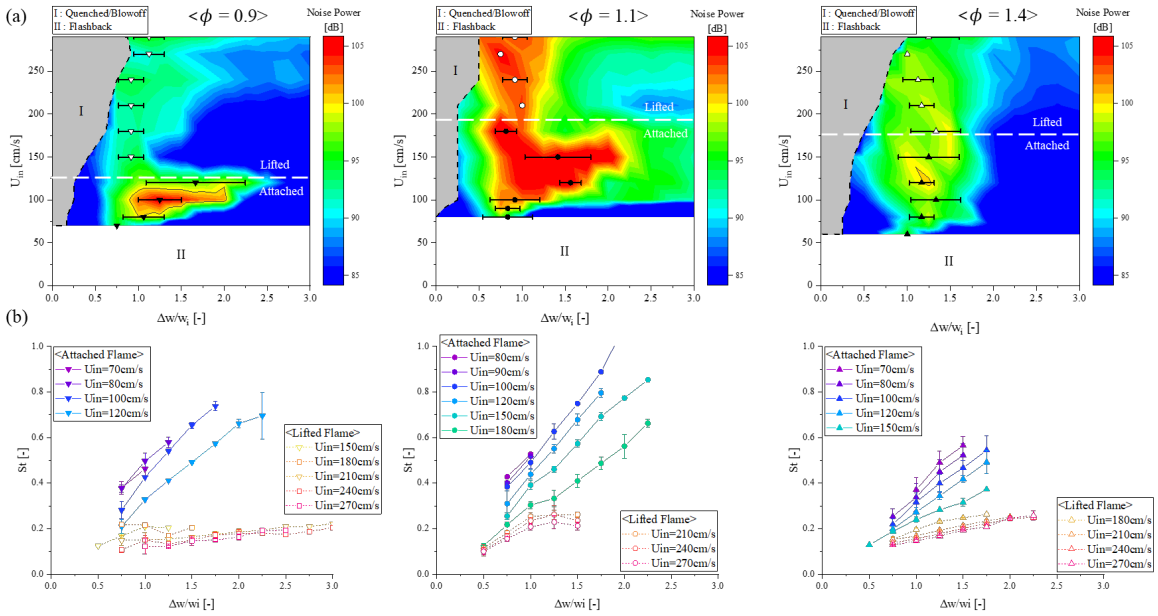

Figure 2: Noise characteristics variation of propane premixed flames ($\phi = 0.9, 1.1, 1.4$) depending on step-width and various inlet velocities ($w_i = 4$ mm); (a) Noise power and (b) Noise frequency scale

Meanwhile, the peak frequency values in the spectrum were also depicted in Fig. 2b, using Strouhal number defined as below.

$$St = \frac{f_1 \Delta w}{U_{in}},$$

where f_1 is the peak frequency corresponding to the maximum power (fundamental frequency) and $\Delta w / U_{in}$ is the characteristic time scale of the BFS configuration.

Overall, St decreased monotonically as the inlet flow velocity increased for the same expansion ratio. However, trends of St were different depending on the flame modes. In the cases of the attached flames (marked solid), St linearly increased with the step-width. Here the frequency did not chanage

significantly with the step-width variation. In the case of the lifted flame (marked hollow), variation of St was much slower. Here the frequency decreased as the step-width or its lift-off height increased. Notably, the slope of St in the low-velocity regime (or attached flames) was the largest in the case of ϕ = 1.1 and smallest in the case of ϕ = 1.4. Thus, the slopes of St were approximately proportional to the LBV. However, the time scale of the lifted flames is affected by additional variables, such as step-width, as the flame position changed with step-width.

Meanwhile, a similarity of $\Delta w_{\max}$ could be found, which corresponds to the step-width range of the strong noise. In Fig. 3a, the relationship between the normalized $\Delta w_{\max}$ with the flame thickness and $\mathrm{Re}_{in} = U_{in} w_i / \nu$ is shown and two regimes were distinguished based on $\mathrm{Re}_{in} \sim 600$ regardless of the fuels or compositions; low-velocity regime and high-velocity regime. In the low-velocity regime, $\Delta w_{\max} / \delta_F$ and Re_{in} had a linear relationship having similar slopes, while the values of $\Delta w_{\max} / \delta_F$ were gathered at around 10 in the high-velocity regime.

These two regimes also had different characteristics in the noise power spectrum, as shown in Fig. 3b. In the low-velocity regime, many harmonic noise peaks were clearly distinguished, and the noise power distribution except for the peaks was much weaker (~ 60 dB). These harmonic peaks are known to be generated by flame oscillation, which is normally induced by the flame-vortex interaction [2,5]. Thus, the flame-vortex interaction might be the dominant source of the combustion noise in this regime.

On the other hand, in the high-velocity regime (lifted flames), harmonic peaks were not clearly distinguished, and the noise power distribution except for the peaks was stronger (~ 90 dB) than the low-velocity regime. In addition, a negative slope was commonly observed at around 300 to 600 Hz, which seems to be generated by the energy dissipation in the turbulent flow, as has been reported [10]. Thus, in this regime, the noise is also generated by turbulence and flame oscillation. Ultimately, the low-velocity regime and the high-velocity regime might correspond to the laminar and turbulent conditions, respectively.

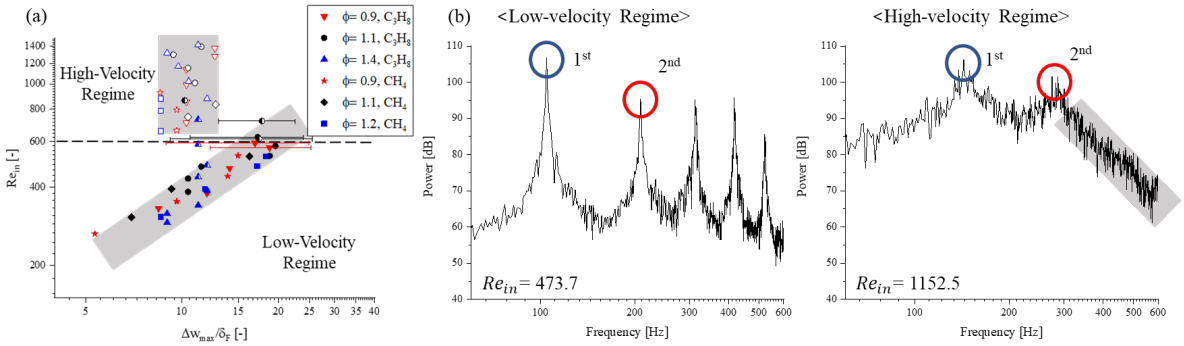

Figure 3: a) Step-width where the maximum power noise occurred for propane and methane flames and b) Noise power spectrum (w_i = 4 mm) for low-velocity regime (ϕ = 0.9, U_{in} = 100 cm/s, $\Delta w / w_i$ = 1.5) and high-velocity regime (ϕ = 1.1, U_{in} = 240 cm/s, $\Delta w / w_i$ = 1)

So far, many cohorent trends of the combustion noise were found. However, it is still unclear which part of the flame generates the noise. Here, the flow field around the inlet nozzle was visualized and synchronized with the flame oscillation to observe flame-vortex interaction.

First, a representative case of the attached flames is shown in Fig. 4. Here, the flame images and flow fields were obtained through ensemble averages based on the fundamental frequency. During the first half of the period, the flame base moved to the surface of the BFS. After that, the base was quenched and a new flame surfacme was re-ignited near the edge of the former flame. Eventually, the new flame

was formed and this process repeatedly occurred with the fundamental frequency. The vortex or the flame oscillation were rarley affected by the step-width variation, and the noise characteristics of the attached flames were maintained regardless of the step-width within a sufficient range (in Fig. 2). Meanwhile, due to the flame-vortex interaction, corrugated flame shape was observed at every cycle (i.e., $t/T = 13/15$). In this case, there must be some positions where the flame passes several times in a cycle and it might lead to the noise peaks of the higher harmonic frequencies.

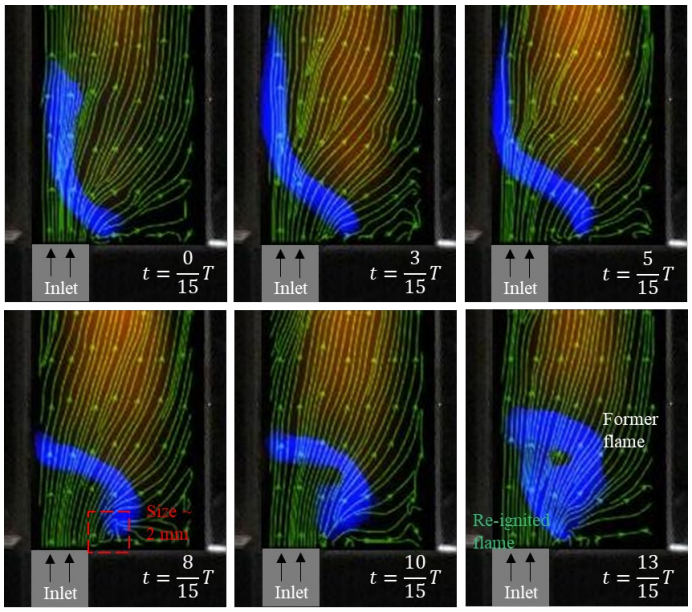

Figure 4: a) Flame oscillation (T= 7.57 ms) with streamline (propane, $\phi = 1.1$, $U_{in} = 120$ cm/s and $\Delta w / w_i = 1.5$)

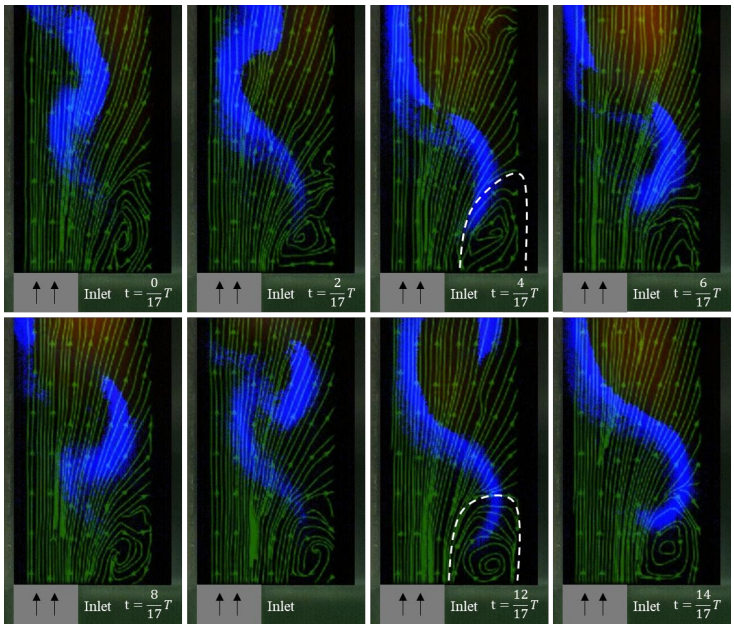

Figure 5: a) Flame oscillation (T= 8.57 ms) with streamline (propane, $\phi = 1.1$, $U_{in} = 210$ cm/s and $\Delta w / w_i = 1$)

On the other hand, a representative case of the lifted flames is also shown in Fig. 5. Since the lifted flame behavior was much more irregular than that of the attached flames, flame images without average were used while the flow fields were still ensemble averaged based on the fundamental frequency. In this case, the flame was stabilized in the shear layer between the recirculation zone (RZ) and the inlet flow. Like the attached flames, flame front quenching and re-ignition were also observed. One notable fact was that the flame-vortex interaction process occurred twice in a period corresponding to the fundamental frequency. In addition, the flame base was occasionally located inside the RZ (i.e., at $t/T = 4/17$ or $t/T = 12/17$). However, the probability of flame propagation into the RZ was not frequent as the attached flames, thus the noise power was generally weaker, as already seen in Fig. 2. This probability could be varied by changing the step-width or the equivalence ratio. It might be critically related to the flame stabilization position and the combustion noise characteristics.

References

[1] Rayleigh. (1878). The explanation of certain acoustical phenomena. Nature 18: 319-321.

[2] Poinsot T, Trouve A, Veynante D, Candel S, Esposito E. (1987). Vortex-driven acoustically coupled combustion instabilities. Journal of Fluid Mechanics, 177: 265-292.

[3] Roberts WL, Driscoll JF. (1991). A laminar vortex interacting with a premixed flame: Measured formation of pockets of reactants. Combust. Flame. 87: 245-256.

[4] Najm HN, Ghoniem AF. (1994). Coupling between vorticity and pressure oscillations in combustion instability. Journal of Propulsion and Power. 10: 6.

[5] Schadow KC, Gutmark TP, Parr TP, Parr DM, Wilson KJ, Crump JE. (1989). Large-Scale Coherent Structures as Drivers of Combustion Instability. Combustion Science and Technology. 64: 4-6, 167-186.

[6] Samaniego JM, Yip B, Poinsot T, Candel S. (1993). Low-frequency combustion instability mechanisms in a side-dump combustor, Combust. Flame. 94: 363-380.

[7] Armaly B, Durst F, Pereira JCF, Schönung B. (1983). Experimental and theoretical investigation of backward-facing step flow. Journal of Fluid Mechanics. 127: 473-496.

[8] Biswas G, Breuer M, and Durst F. (2004). Backward-facing step flows for various expansion ratios at low and moderate Reynolds numbers. ASME. J. Fluids. Eng. 126: 362–374.

[9] Thielicke W, Sonntag R. (2021) Particle Image Velocimetry for MATLAB: Accuracy and enhanced algorithms in PIVlab. Journal of Open Research Software 9: 12.

[10] Abugov DI, Obrezkov OI, Acoustic noise in turbulent flames. (1978). Combust. Explos. Shock Waves 14: 606–612.